Benzoyl-CoA reductase (dearomatizing), a key enzyme of anaerobic aromatic metabolism. Study of adenosinetriphosphatase activity, ATP stoichiometry of the reaction and EPR properties of the enzyme

Boll, M.; Albracht, S.P.J.; Fuchs, G.

Publication date
1997

Published in
European Journal of Biochemistry

Eur. J. Biochem. 244, 840–851 (1997)

Benzoyl-CoA reductase (dearomatizing), a key enzyme of anaerobic aromatic metabolism

A study of adenosinetriphosphatase activity, ATP stoichiometry of the reaction and EPR properties of the enzyme

Matthias BOLL[1], Simon S. P. ALBRACHT[2] and Georg FUCHS[1]

[1] Mikrobiologie, Institut Biologie II, Universität Freiburg, Germany
[2] E. C. Slater Institute, Biochemistry/FS, University of Amsterdam, The Netherlands

(Received 5 November 1996/15 January 1997) – EJB 96 1641/4

An enzyme was recently described, benzoyl-CoA reductase (dearomatizing), which catalyses the ATP-driven reduction of the aromatic ring of benzoyl-CoA yielding a non-aromatic CoA thioester, ADP and phosphate [Boll, M. & Fuchs, G. (1995) *Eur. J. Biochem. 234*, 921–933]. The 170-kDa enzyme consists of four different subunits and contains approximately 12 Fe and acid-labile sulfur/mol. Benzoyl-CoA reductase exhibits ATPase activity in the absence of substrate. It is shown that only the reduced form of this iron-sulfur protein has ATPase activity. ATPase activity is reversibly lost when the enzyme is oxidized by thionine; reduction of the enzyme fully restores ATPase and ring-reduction activity. 2 mol ATP are hydrolyzed/2 mol electrons transferred in the course of the reaction. The product ADP acts as competitive inhibitor (K_i = 1.1 mM) for ATP in benzoyl-CoA reduction; ADP inhibits ATPase activity to the same extent as ring-reduction activity. EPR investigation of the dithionite-reduced enzyme suggested the presence of two separate [2Fe-2S] clusters and two interacting [4Fe-4S] clusters. Addition of MgATP to the reduced enzyme resulted in a new isotropic signal at g = 5.15 and a weak signal at g = 12; in controls with MgADP only a minor signal at g = 5.15 was observed. The positions, shapes and temperature dependencies of these MgATP-induced signals are indicative for excited states of a S = 7/2 spin multiplet. The [2Fe-2S] signals were not affected by ATP, but one of the [4Fe-4S] clusters became slowly oxidized. Addition of both benzoyl-CoA and MgATP resulted in a major oxidation of the iron-sulfur clusters accompanied by the appearance of some minor signals of unknown origin in the g = 2.037–1.96 region. Neither the benzoyl-CoA plus MgATP-oxidized nor the thionine-oxidized enzyme showed the ATP-dependent formation of the high-spin signals of the reduced enzyme. At present we hypothesize that the S = 7/2 signal is due to an ATP-induced change of one of the [4Fe-4S] clusters.

The data suggest that hydrolysis of MgATP is required to activate the enzyme; in the absence of substrate the energy involved in this activation dissipates. MgATP-driven formation of this excited state of the reduced enzyme rather than transfer of electrons from the reduced enzyme to the aromatic substrate appears to be the rate-limiting step in the catalytic cycle. We suggest that the excited state is required to overcome the high activation energy associated with the loss of the aromatic character and/or to render ring reduction irreversible.

Keywords: benzoyl-CoA reductase; high-spin; iron-sulfur protein; nitrogenase; (*R*)-2-hydroxyglutaryl-CoA dehydratase.

The metabolism of aromatic compounds requires molecular oxygen as cosubstrate for ring hydroxylation and cleavage. Yet, a number of bacteria are known to degrade various aromatic growth substrates to CO_2 even under anoxic conditions. It has been established that those bacteria are able to reduce the aromatic ring first and subsequently oxidize the alicyclic product formed. The peripheric metabolism of many, though not all, mononuclear aromatic compounds channels into the central intermediate benzoyl-CoA. Benzoyl-CoA is reduced by the key enzyme benzoyl-CoA reductase (dearomatizing) [1–5].

This enzyme has recently been purified from the denitrifying bacterium *Thauera aromatica* strain K172 and studied. It is an iron-sulfur protein with approximately 10–12 mol Fe and acid-labile sulfur/mol. So far, all preparations contained in addition approximately 0.3 mol of an unidentified flavin compound/mol enzyme. The 160–170-kDa protein consists of four subunits of 48, 45, 38 and 32 kDa. The enzyme catalyses the two-electron reduction (Fig. 1) of the aromatic ring of benzoyl-CoA, of NH_2OH and N_3^-; the products of these reduction reactions most likely are cyclohex-1,5-diene-1-carboxyl-CoA, $NH_4^+ + H_2O$, and $N_2 + NH_4^+$, respectively (Fig. 1). Yet, the exact stoichiometry of the reaction and the nature of the products remain to be identified. All these reduction reactions require the hydrolysis of ATP giving ADP + P_i; the stoichiometry observed was 2–

Correspondence to G. Fuchs, Mikrobiologie, Institut Biologie II, Schänzlestr. 1, D-79104 Freiburg, Germany
Fax: +49 761 2032626.

Abbreviations. Ado*P*[CH_2]*PP*, adenosine 5′-[β,γ-methylene]triphosphate; Ado*P*[NH]*PP*, adenosine 5′-[β,γ-imido]triphosphate.

Enzymes. Benzoyl-coenzyme A reductase (dearomatizing) (EC 1.3.–.–); nitrogenase (EC 1.18.6.1), (*R*)-2-hydroxyglutaryl-CoA dehydratase (EC 4.2.1.–).

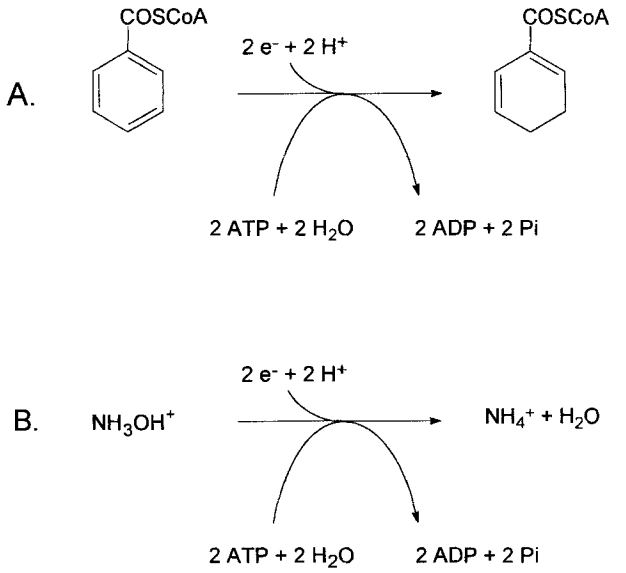

Fig. 1. Reactions catalyzed by benzoyl-CoA reductase (dearomatizing). The ATP stoichiometry was at issue, the products formed were deduced from the amount of electrons consumed (NH_2OH) and from NMR studies of products formed in cell extract (benzoyl-CoA). ADP was identified as product of ATP hydrolysis [4].

4 mol ATP hydrolyzed/mol substrate. In the absence of substrate, ATP is hydrolyzed to ADP and P_i. Both reductase and ATPase activities are irreversibly and rapidly lost under aerobic conditions.

The aim of this work was to address the following questions: (a) Is ATP hydrolyzed by the reduced or the oxidized enzyme or by both? (b) What is the exact stoichiometry of ATP hydrolyzed per two electrons transferred in the reaction? (c) What are the EPR characteristics of the iron-sulfur clusters? (d) Do the substrates MgATP and benzoyl-CoA have any effect on the EPR spectra, and if so, can something be learned about rate-limiting steps and the role of MgATP in electron transfer? (e) Which enzyme states can be discerned on the basis of their EPR properties and do they allow us to propose a catalytic cycle?

We show that 2 ATP/2 electrons are hydrolyzed. A MgATP-induced signal is described which is attributed to the exited state of a $S = 7/2$ high-spin system of the reduced enzyme.

MATERIALS AND METHODS

Materials and bacterial strain. Chemicals were of analytical grade. Biochemicals were from Sigma or Gerbu. Benzoyl-CoA was synthesized from CoA and benzoic acid anhydride according to the method of Schachter and Taggart [6]. [*phenyl*-^{14}C]Benzoyl-CoA was enzymatically synthesized from [*phenyl*-^{14}C]benzoate (American Radiolabeled Chemicals Inc./Biotrend Chemikalien GmbH) and CoA with enriched benzoate-CoA ligase from *T. aromatica* strain K172 as described earlier [7]. All LC and FPLC materials and equipment for enzyme purification were obtained from Pharmacia or BioRad. HPLC materials and equipment were from Merck. *Thauera aromatica* strain K172 (DSM 6984) was isolated in our laboratory [8] and has been deposited in the *Deutsche Sammlung von Mikroorganismen* (Braunschweig, Germany) [9].

Growth of bacterial cells. *T. aromatica* strain K172 was grown anoxically at 28 °C in a mineral salt medium. 4-Hydroxybenzoate or 2-amino-benzoate and nitrate served as sole sources of energy and cell carbon. Benzoyl-CoA reductase is expressed during growth with both substrates. Continuous feeding of the substrates, cell harvesting, storage and preparation of cell extracts were performed as described [8].

HPLC-analysis of CoA-thioesters and adenine nucleotides. *CoA-thioesters.* HPLC of non-hydrolyzed CoA-thioesters was performed both for purity control of synthesized benzoyl-CoA and for quantitative analysis of the products formed from benzoyl-CoA by enzyme catalysis. Sample preparation was as previously described [4]. HPLC analysis was carried out by separation of the CoA-thioesters on a Lichrosphere RP-C18 column (25 cm×0.4 cm, Merck) using an eluent of 11% (by vol.) acetonitrile in 50 mM aqueous potassium phosphate, pH 6.7; the elution rate was 1 ml/min. Quantitative detection of the CoA-thioesters was performed with an ultraviolet-visible detector at 260 nm.

Adenine nucleotides. For quantitative HPLC analysis of adenine nucleotides the protein-free samples were applied to a 1-ml Mono Q FPLC-anion exchange chromatography column as described earlier [4]. A linear 0 to 500 mM KCl gradient in 50 mM potassium phosphate, pH 6.7, was used for separation of AMP (retention time 1.8 min), ADP (7.5 min) and ATP (11.8 min). Ultraviolet-visible spectrometric detection was at 260 nm.

Enzyme assays. All enzyme assays, also when performed with thionine-oxidized enzyme, were prepared under strictly anaerobic conditions in stoppered cuvettes or tubes with N_2/H_2 (95:5, by vol.) as gas phase. All additions and sampling were performed with gas-tight syringes. Assay temperature was 37 °C.

Benzoyl-CoA reductase activity: oxidation of reduced methyl viologen. The MgATP- and benzoyl-CoA- or hydroxylamine-dependent oxidation of dithionite-reduced methyl viologen was determined in a continuous spectrophotometric assay at 730 nm as previously described [4]. To prevent loss of ATP before starting the reaction due to ATPase activity, the reaction was usually started by adding ATP.

ATPase activity: quantitative HPLC-analysis of ADP formed from ATP. The hydrolysis of ATP to ADP and P_i catalyzed by benzoyl-CoA reductase in the absence of a reducible substrate was carried out as previously described [4]. The standard 1-ml assay contained, if not otherwise stated, 150 mM Mops/KOH, pH 7.3, 5–10 mM ATP, 10–20 mM $MgCl_2$, 5 mM sodium dithionite and 5–10 μM purified benzoyl-CoA reductase (1–2 mg protein). In the time-course experiments 100-μl samples were retrieved at intervals. Protein was denatured by adding 10 μl 10% (mass/vol.) $HClO_4$, followed by centrifugation and addition of 2 μl 5 M K_2CO_3 to give pH 6–7. After centrifugation the clear supernatants were applied to a Mono Q FPLC-column (1 ml, Pharmacia) for adenine nucleotide analysis. For examination of the effect of acetylene on ATPase activity, saturated, oxygen-free stock solutions of the gases were prepared as described [4]. 10–50 μl of the saturated solution were added to the standard 1-ml ATPase activity assay and incubated together with the enzyme for 5 min. For examination of the effects of thionine-oxidation of benzoyl-CoA reductase the 1-ml assay mixture did not contain dithionite and was anaerobically oxidized as described below. Re-reduction of the enzyme was performed by adding aliquots of a 100 mM dithionite stock solution to the enzyme assay, resulting in a final dithionite concentration of at least 5 mM. All ATPase assays were started by addition of ATP (50–100 μl from an anaerobic 100 mM stock solution in 150 mM Mops/KOH, pH 7.3).

Purification of benzoyl-CoA reductase. The purification was carried out at 4 °C under strictly anaerobic conditions in a glove box with N_2/H_2 (95:5, by vol.) as gas phase. All buffers contained 0.5 mM dithionite and 1 mM dithioerythritol as reducing agents. Preparation started with extract from 200 g cells (wet

mass). The purification procedure used DEAE and Mono Q anion-exchange chromatography, chromatography on hydroxyapatite and gel filtration, as described previously [4]. Benzoyl-CoA reductase activity was determined by the continuous spectrophotometric assay as described above [4]. The enzyme was enriched 35-fold to apparent homogeneity.

Thionine-oxidation of benzoyl-CoA reductase. The effect of the oxidation state of benzoyl-CoA reductase on both ATPase activity and EPR properties was studied as follows. All assays were performed under anaerobic conditions. The enzyme as isolated contained 0.5 mM dithionite and was mostly in the reduced state. To obtain oxidized enzyme, the solutions were titrated with an anaerobically prepared saturated solution of thionine in 150 mM Mops/KOH, pH 7.3, and 4 mM $MgCl_2$ until the colour of the solution remained blue. For determination of benzoyl-CoA reductase activity aliquots of the thionine-oxidized enzyme were directly applied to the spectrophotometric assay as described [4], containing 0.5–0.6 mM dithionite-reduced methyl viologen. After this procedure there was still enough reduced methyl viologen in the assay for benzoyl-CoA reduction. Re-reduction with dithionite in the ATPase assay was performed as described above.

Determination of stoichiometry of substrate-dependent ATP-hydrolysis. *Quantitative HPLC analysis of substrate consumption and product formation.* The molar ratio of ATP hydrolyzed/benzoyl-CoA reduced catalyzed by purified benzoyl-CoA reductase was determined. This was achieved by quantitative HPLC/analysis of the consumption of ATP and benzoyl-CoA and of the formation of ADP and non-aromatic products. The assay was performed under anaerobic conditions in a stoppered tube at 37 °C. The 1.35-ml assay contained 150 mM Mops/KOH, pH 7.3, 10 mM $MgCl_2$, 5 mM dithionite, 1.025 μmol benzoyl-CoA, 9 kBq [*phenyl*-^{14}C]benzoyl-CoA and 2 μmol (0.35 mg) purified benzoyl-CoA reductase. The reaction was started by adding 7.5 μmol ATP. At intervals 200-μl samples were taken and added to 20 μl 10% (mass/vol.) $HClO_4$ on ice. After centrifugation of the denatured enzyme, 4 μl of 5 M K_2CO_3 were added to give pH 6–7, followed by centrifugation. For detection of adenine dinucleotides 25 μl of the protein-free sample was applied to a Mono Q column (1 ml, Pharmacia); for separation and detection of the CoA-thioesters 40 μl was applied to a Lichrosphere C-18 RP-column (1 ml, Merck; retention time for benzoyl-CoA, 7.9 min). The amounts of substrates and products were quantified by (a) integration of the HPLC peaks detected at 260 nm and comparison of the areas with standards; (b) calculation of the concentrations of ATP, ADP and benzoyl-CoA from their absorption coefficients (ATP and ADP ε_{260} = 15.4 mM^{-1} cm^{-1} [10], benzoyl-CoA ε_{260} = 21.3 mM^{-1} cm^{-1} [11]); the absorption coefficient of 21.3 mM^{-1} cm^{-1} was also assumed for other CoA thioesters; (c) determination of the amount of radioactivity in the individual 1–1.5 ml HPLC peaks by liquid-scintillation counting. The molar amounts of aromatic substrate and non-aromatic products were calculated from the known specific radioactivity of [^{14}C]benzoyl-CoA. All quantitation methods gave similar results.

The molar ratio of ATP hydrolyzed/benzoyl-CoA or hydroxylamine reduced by purified benzoyl-CoA reductase was also extrapolated by determining the amount of ADP formed after completion of substrate reduction. To this end different amounts of benzoyl-CoA or hydroxylamine (0.5 μmol and 1 μmol/ml assay) were added. The completion of substrate reduction was manifested by the levelling off of ADP formation. After starting the reaction by adding ATP, 100-μl samples were periodically taken and analyzed for ATP and ADP on a Mono Q anion-exchange column as described above.

ADP-Inhibition assays. The competitive inhibitory effect of MgADP on benzoyl-CoA reductase was investigated for both benzoyl-CoA reductase activity and ATPase activity.

Benzoyl-CoA reductase activity. The inhibitory effect of MgADP on benzoyl-CoA reductase activity was determined in the continuous spectrophotometric assay [4] following at 730 nm the ATP-dependent and substrate-dependent oxidation of reduced methyl viologen. The enzyme was incubated for 5 min at 37 °C with 0–4 mM MgADP in the absence of ATP but in the presence of all other substrates. The reaction was then started by adding ATP to final concentrations of 0.4–3.4 mM. Extrapolation of the K_i value was by Dixon plot analysis.

ATPase activity. The inhibitory effect of MgADP on ATPase activity was determined with the standard ATPase assay as described above. The enzyme was incubated under reducing conditions with 5 mM dithionite and 1–5 mM ADP in the absence of ATP and any reducible substrate. The reaction was started by adding 5 mM ATP, samples were taken at intervals and applied to a Mono Q column for ADP and ATP determination as described. ATPase activity in the absence of ADP served as control (100% activity).

Inhibition assays for ATP analogs. The inhibition or inactivation of benzoyl-CoA reductase by the ATP analogs adenosine 5′-[β,γ-methylene]triphosphate (Ado*P*[CH_2]*PP*) and adenosine 5′[β,γ-imido]triphosphate (Ado*P*[NH]*PP*) was assessed with the methyl viologen-oxidizing spectrophotometric assay at 730 nm [4]. Two different methods were used. The standard assay was started with 5 mM ATP and the linear decrease of absorbance at λ of 730 nm was followed for approximately 2 min until A_{730} was about 0.8–1.0. At this point the ATP analog was anaerobically added to the assay and the gradually decreasing enzyme activity was recorded. If the time-dependent inactivation curve was to be observed, the rates at different time-points were extrapolated from the first derivative of the recorder plot. Alternatively, the enzyme was incubated with the ATP analog for different times in the absence of ATP but in the presence of benzoyl-CoA (0.5 mM). The reaction was started by addition of 5 mM ATP. Enzyme activities were determined immediately upon ATP addition and after 3 min.

Electron paramagnetic resonance spectroscopy. *Sample preparation.* All samples for EPR analysis were handled under strictly anaerobic conditions in a glove box with N_2/H_2 (95:5, by vol.) gas phase at 20 °C. The investigated enzyme preparations were of highest purity or, since no differences in EPR spectra were detectable, with preparations of the hydroxyapatite purification step (purity 80–90%). The samples were anaerobically concentrated with Microsep-CCR microconcentrators (exclusion limit of 50 kDa; Filtron) to a protein content of 8–15 mg/ml. After 1:10 dilution of the obtained enzyme preparations with 150 mM Mops/KOH, pH 7.3, 10–20 mM $MgCl_2$ and 0.5 mM dithionite (buffer A) the samples were concentrated again. This procedure was repeated twice. All preparations were anaerobically transferred to EPR tubes in 300-μl portions and immediately frozen in liquid nitrogen or, if needed, in heptane cooled to the viscous state (200 K) with liquid nitrogen.

Reduced and oxidized enzyme. For all EPR measurements of the reduced enzyme, 2–5 mM dithionite was added to the enzyme preparation in buffer A. The oxidation of enzyme was performed with an anaerobically prepared, saturated thionine stock solution as described above.

ATPase activity. For EPR investigation of benzoyl-CoA reductase in the steady state of ATPase activity, 40 μl of an anaerobically prepared, neutralized 250 mM ATP solution in 150 mM Mops/KOH, pH 7.3, was added to 960 μl of an enzyme preparation in buffer A containing 5 mM dithionite. The enzyme solution (12 mg/ml) was anaerobically incubated at 20 °C; at t =

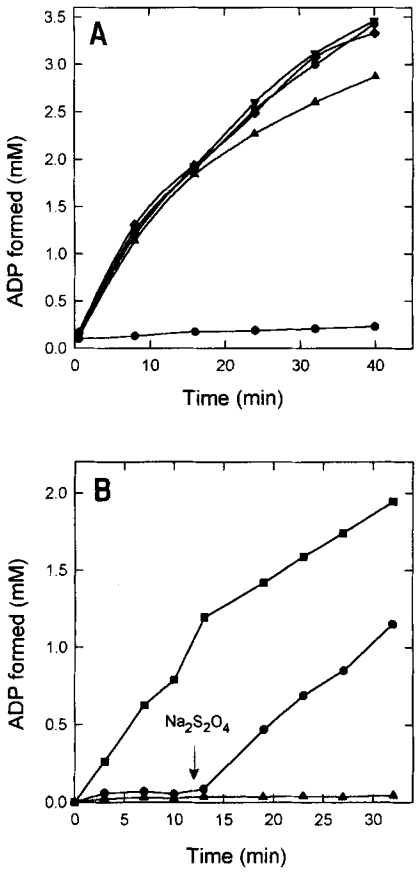

Fig. 2. ATPase activity of benzoyl-CoA reductase. (A) ATPase activity of the thionine-oxidized enzyme (●) and of the dithionite-reduced enzyme. (▲) Enzyme as isolated in the presence of 0.25 mM dithionite, (♦) plus 1 mM dithionite, (▼) plus 5 mM dithionite, (■) plus 20 mM dithionite. (B) Reversibility of loss of ATPase activity upon enzyme oxidation and subsequent reduction of the enzyme. ATPase activity of the oxidized enzyme and after reduction by dithionite (●). Controls: ATPase activity of thionine-oxidized enzyme (▲) and of dithionite-reduced enzyme (■). The arrow marks the addition of 5 mM dithionite. For experimental conditions, see Materials and Methods.

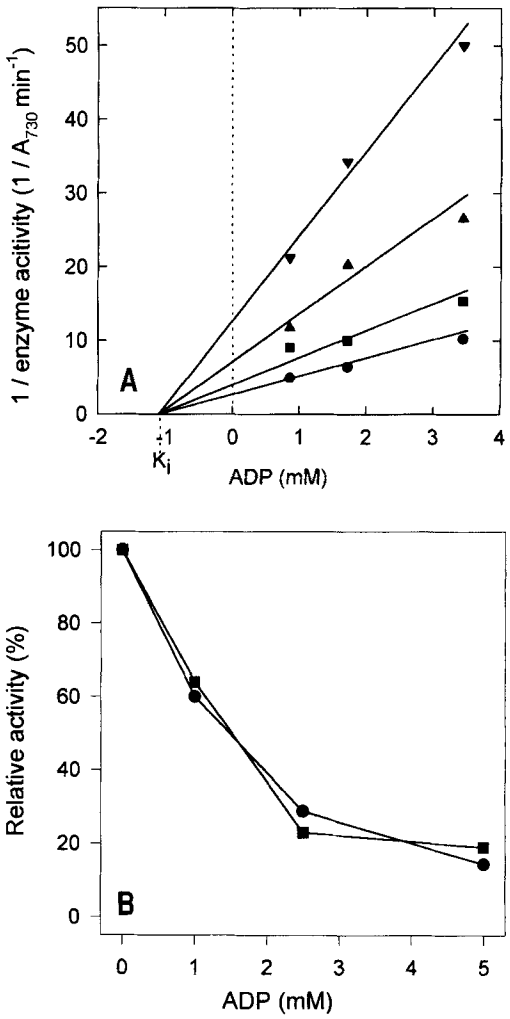

Fig. 3. Inhibition of benzoyl-CoA reductase and ATPase activity by ADP. (A) Inhibition of benzoyl-CoA reductase activity by different concentrations of ADP with (▼) 0.43 mM, (▲) 0.85 mM, (■) 1.7 mM and (●) 3.4 mM ATP as substrate. The data are represented as Dixon-plot. (B) Comparison of the inhibitory effect of ADP on benzoyl-CoA reductase activity (●) and on ATPase activity (■) of benzoyl-CoA reductase. In both assays 5 mM of ATP was present. 100% activity corresponded to 0.84 U/mg protein for benzoyl-CoA reductase activity and 0.12 U/mg protein for ATPase activity (1 U ATPase activity is defined as hydrolysis of 1 μmol/min ATP to ADP). For further conditions see Materials and Methods.

0.5 min, 5 min and 10 min, 300-μl samples were quickly transferred to an EPR tube and immediately frozen in cold (200 K) heptane.

Benzoyl-CoA reductase activity. EPR investigation of benzoyl-CoA reductase in the steady state of benzoyl-CoA reductase activity was performed in buffer A containing 10 mM dithionite and 2 mM benzoyl-CoA or hydroxylamine. The reaction was started by adding 10 mM ATP to the reaction mixture. After incubation for 30 s at 20 °C the enzyme solution was transferred to an EPR tube and immediately frozen in cold heptane.

EPR system. EPR measurements at X-band (9 GHz) were obtained with a Bruker ECS 106 EPR spectrometer at a field-modulation frequency of 100 kHz. Cooling of the sample was performed with an Oxford Instruments ESR 900 cryostat with a ITC4 temperature controller. The sample-temperature indication from this instrument was correct from 4.2 K to 100 K within ±2% as ascertained from the Curie dependence of a copper standard (10 mM $CuSO_4 \cdot 5\,H_2O$, 2 M $NaClO_4$, 10 mM HCl). The magnetic field was calibrated with an AEG Magnetic Field Meter. The X-band frequency was measured with an HP 5350B microwave frequency counter. The microwave power incident to the cavity was measured with an HP 432 B power meter (260 mW at 0 dB). Quantification of EPR signals was carried out by direct double integration of the experimental spectra [15].

Other determinations. Protein was determined by the Bradford method [12]. ^{14}C radioactivity was determined by liquid-scintillation counting (Betamatic 1, Kontron) using external standardization. SDS/PAGE (10% polyacrylamide) for purity control of the enzyme preparations were performed as described by Laemmli [13]. Proteins were visualized by Coomassie blue staining [14].

RESULTS

ATPase activity of benzoyl-CoA reductase. In our previous work benzoyl-CoA reductase was always studied in the reduced state since this oxygen-sensitive enzyme had to be purified in the presence of dithionite. Likewise the ATPase activity was only measured with the reduced enzyme. To inspect the effect of the redox state on enzyme activity, benzoyl-CoA reductase was oxidized under anaerobic conditions with an excess of the mild

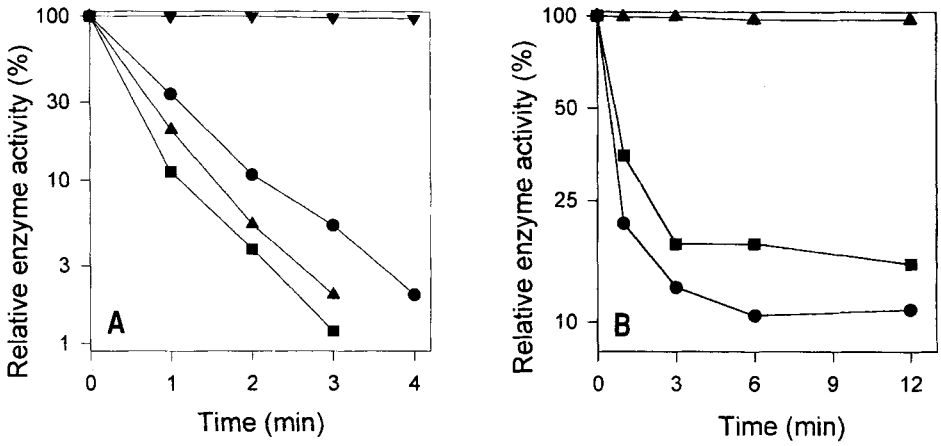

Fig. 4. Inactivation of benzoyl-CoA reductase activity by Ado*P*[NH]*PP*. (A) Time-course of loss of enzyme acitivity after adding different amounts of Ado*P*[NH]*PP* to the assay. The decreasing relative enzyme activities were determined after different times upon Ado*P*[NH]*PP* addition to the complete spectrophotometric assay at λ = 730 nm (5 mM MgATP and 0.5 mM benzoyl-CoA). Enzyme activities upon addition of (●) 40 μM Ado*P*[NH]*PP*, (▲) 200 μM Ado*P*[NH]*PP* and (■) 400 μM Ado*P*[NH]*PP*; (▼) control without Ado*P*[NH]*PP*. (B) Time-course of loss of enzyme activity after different periods of prior incubation of the enzyme with Ado*P*[NH]*PP* in the absence of ATP. Initial enzyme activities (●) subsequently upon ATP addition and (■) 3 min after start of the reaction. (▲) Control without Ado*P*[NH]*PP*. The reaction was started by addition of ATP. 100% refers to an enzyme activity of 550 nmol benzoyl-CoA reduced per min/ml assay.

oxidizing agent thionine (E_0' = 60 mV). After re-reduction of the oxidized enzyme with dithionite or reduced methyl viologen, 80–90% of the original benzoyl-CoA reductase activity was recovered. Hence, the enzyme can reversibly be oxidized; this allowed us to examine ATPase activity as a function of the redox state of the enzyme.

Addition of excess dithionite to the enzyme as isolated, which was in the reduced state, did not result in a variation of ATPase activity. Oxidation by thionine, however, resulted in a virtually complete loss of ATPase activity (Fig. 2 A). This loss of ATPase activity was reversible (Fig. 2 B). Reduction of the oxidized enzyme with dithionite resulted in an immediate resumption of full ATPase activity. These experiments showed that only the reduced enzyme has ATPase activity and that ATPase activity can reversibly be turned off by oxidation.

Inhibition of enzyme activities by ADP and non-hydrolyzable ATP analogs. The effects of the product ADP and non-hydrolyzable ATP analogs on benzyol-CoA reductase activity, and the effect of MgADP on ATPase activity were investigated. MgADP inhibited both reactions reversibly. Analysis of the data by Dixon plot (Fig. 3 A) indicated that MgADP acts as competitive inhibitor of MgATP (K_i = 1 mM) in the reductase reaction. MgADP also inhibited ATPase activity to the same extent as benzoyl-CoA reductase activity (Fig. 3 B).

Ado*P*[CH_2]*PP* had only little effect on benzoyl-CoA reductase activity and only at high concentration (> 10 mM) when 5 mM MgATP was present. In contrast, Ado*P*[NH]*PP* acted as potent inactivating compound of benzoyl-CoA reductase activity. Inactivation was detectable at 10 μM in the presence of 5 mM MgATP. The time-dependent loss of benzoyl-CoA reductase activity during incubation with different concentrations of Ado*P*[NH]*PP* is shown in Fig. 4. In Fig. 4A Ado*P*[NH]*PP* was added to the running benzoyl-CoA reductase assay, and the remaining methyl viologen oxidation rate was extrapolated at different times. The graph shows a semi-logarithmic plot of residual activity versus time. In Fig. 4 B the enzyme was incubated for different times with Ado*P*[NH]*PP* in the absence of ATP; then the reaction was started with 5 mM ATP and the residual initial enzyme activity was determined. Enzyme activities measured 3 min after ATP addition were 10–20% higher than the initial activity. This suggests a slow reactivation of the enzyme in the presence of ATP.

Table 1. Stoichiometry between ATP hydrolysis and benzoyl-CoA reduction. ATP, ADP and benzoyl-CoA were analyzed by quantitative HPLC. Note that 2.1–2.2 mol electrons are transferred to benzoyl-CoA [4]. Besides the postulated main product cyclohex-1,5-diene-1-carboxyl-CoA (requiring 2-electron reduction), always a small amount (10% of products) of cyclohex-1-ene-1-carboxyl-CoA (requiring 4-electron reduction) was observed. This explains a stoichiometry which is slightly higher than 2 ATP/benzoyl-CoA.

ADP formed	Benzoyl-CoA consumed	Molar ratio ADP formed/ benzoyl-CoA consumed
nmol		
0	0	
371	163	2.27
747	334	2.23
1036	469	2.21
1381	622	2.22
2232	999	2.23
2732	1016	2.68

Stoichiometry of ATP hydrolysis/electron transferred. The determination of an exact ATP/2e^- stoichiometry during benzoyl-CoA reduction with the coupled spectrophotometric assay for ADP formation was doubtful, since the enzyme hydrolyzed ATP in the absence of substrate. The end point of substrate-dependent ADP formation was difficult to detect because of continuing ADP formation after all substrate was consumed. Furthermore, it had to be assessed whether substrate-dependent ATP hydyrolysis was accompanied by substrate-independent ATPase activity or not.

We reassessed the stoichiometry by direct determination of substrates and products by HPLC (Table 1). At the beginning of the reaction, when excess benzoyl-CoA and MgATP were present, a linear relation between benzoyl-CoA consumption and ADP formation was found. At all time-points before completion of benzoyl-CoA reduction the stoichiometry was constant and

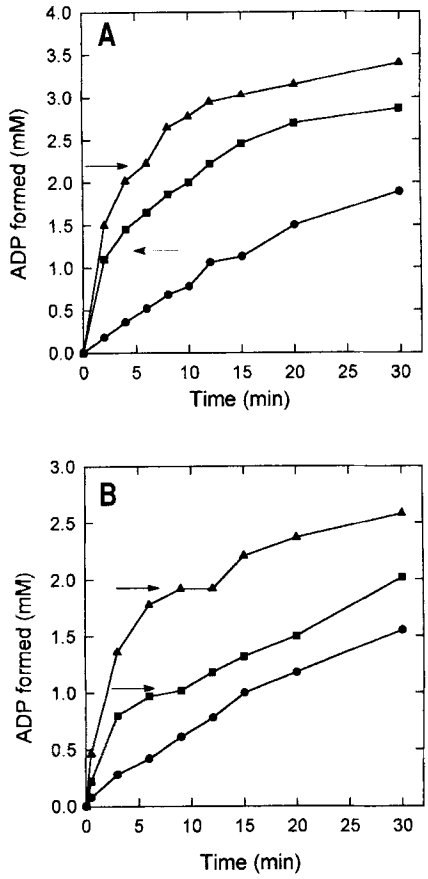

Fig. 5. Stoichiometry of ATP consumption during the reduction of NH_2OH and of benzoyl-CoA. (A) Formation of ADP at different concentrations of benzoyl-CoA initially present (▲) 1 μmol benzoyl-CoA/ml assay, (■) 0.5 μmol benzoyl-CoA/ml assay, (●) without benzoyl-CoA. (B) Formation of ADP at different concentrations of NH_2OH initially present. (▲) 1 μmol NH_2OH/ml assay, (■) 0.5 μmol NH_2OH/ml assay, (●) without NH_2OH. Note that both substrates were consumed within the first 10 min of incubation. The arrows mark the point of complete consumption of the reducible substrate.

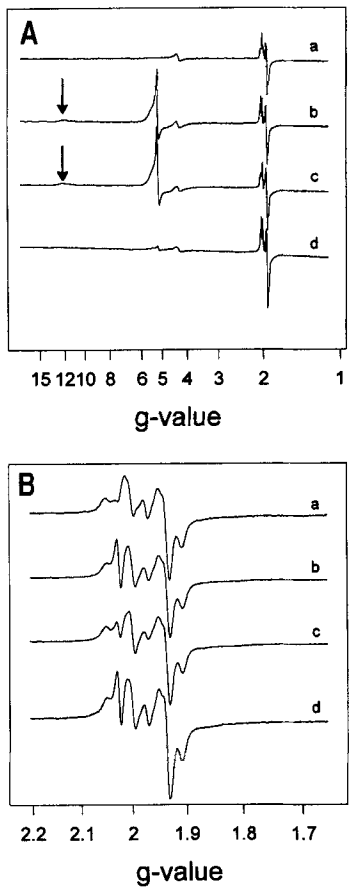

Fig. 6. Effect of ATP on the EPR spectra of completely dithionite-reduced benzoyl-CoA reductase at 25 K. (A) Large spectral region showing the appearance of new signals at $g = 5.15$ and $g = 12$. The arrows point to the appearance of a second signal at $g = 12$. (a) Control without ATP, (b) after 0.5 min, (c) after 5 min, (d) after 10 min incubation with 10 mM ATP. (B) Small spectral region of the spectra in (A) showing the signals of the [2Fe-2S] clusters. The enzyme (12 mg/ml) was incubated at 25 °C with 10 mM MgATP in the presence of 5 mM dithionite. Samples were taken periodically and frozen. EPR conditions: microwave frequency, 9415–9418 MHz; modulation frequency, 100 kHz; modulation amplitude, 1.27 mT; microwave power, 20 dB; temperature, 25 K.

amounted to 2.2 ADP formed/1 benzoyl-CoA reduced. Since the experimentally determined stoichiometry was 2.1 electrons transferred/benzoyl-CoA consumed [4], the stoichiometry of ADP formed/benzoyl-CoA reduced is close to 2.0. Only after virtually complete consumption of benzoyl-CoA, the ADP/benzoyl-CoA ratio increased, probably due to uncoupled ATPase activity.

We also determined the amount of ADP formed with different amounts of benzoyl-CoA and hydroxylamine added, after the reaction had come to completion. Fig. 5 shows the time-dependent ADP formation upon reduction of different amounts of benzoyl-CoA (Fig. 5A) and hydroxylamine (Fig. 5B). The hydroxylamine-dependent formation of ADP clearly proceeds in a biphasic manner (Fig. 5B). The kinks in the graphs (marked by arrows in Fig. 5) are interpreted as the points where the enzyme shifts from substrate-dependent to uncoupled ATPase activity. Substrate-dependent ADP formation should decrease when the substrate concentration decreases below a threshold value defined by the K_m value. The K_m values for NH_2OH (150 μM) and benzoyl-CoA (15 μM) differ by a factor of 10. Therefore, the enzyme should operate longer at non-saturating conditions with NH_2OH than with benzoyl-CoA. Accordingly, the time period, where the rate of substrate-dependent ADP formation was below the rate of uncoupled ADP formation, is longer with NH_2OH than with benzoyl-CoA. As shown in Fig. 5, 0.5 mM and 1 mM of benzoyl-CoA and NH_2OH were added which were consumed after 3 min and 5 min. With both substrates a levelling off of the substrate-dependent ADP-formation was observed when 1 mM and 2 mM ADP were formed, respectively. Hence, two independent determinations clearly indicate a stoichiometry of 2 ATP hydrolyzed to ADP/2 electrons transferred in the reduction, irrespective of whether the substrate was benzoyl-CoA or hydroxylamine.

Thus far, these values were not corrected for ADP formation in the absence of substrate. We will show by EPR experiments that the steady-state form of the enzyme in the presence of all substrates (i.e. reductant + MgATP + benzoyl-CoA or hydroxylamine) is in the oxidized state. It was shown (Fig. 2) that the oxidized enzyme has no ATPase activity. Therefore, from these two observations, we conclude that during the reduction reaction no substrate-independent ADP formation occurred. Hence, the observed stoichiometries need not be corrected for uncoupled ATPase activity, as long as substrate is present. Only after virtually complete substrate consumption does ATPase activity have to be taken into account. Substrate-independent ATPase activity in any case was approximately 15% of the initial rate of substrate-dependent ADP formation.

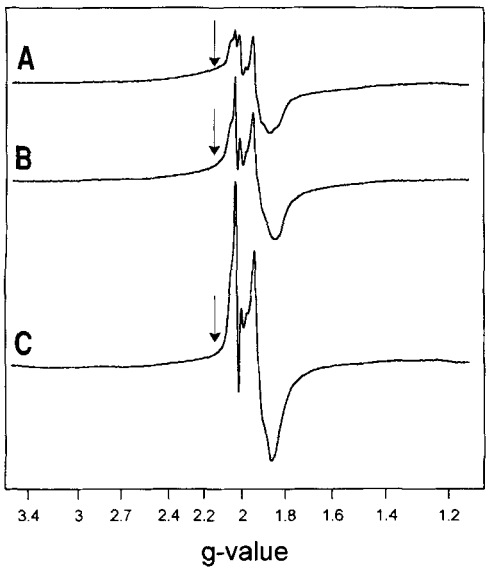

Fig. 7. Effect of ATP on the EPR spectra of dithionite-reduced benzoyl-CoA reductase at 10 K (12 mg/ml). EPR spectra of the reduced enzyme (A) without ATP, (B) after 0.5 min incubation with ATP, (C) after 10 min incubation. The arrows point to the spectrum region of the broad wings in the EPR spectra which disappear after prolonged incubation with ATP. Sample preparation was as in Fig. 6. EPR conditions: microwave frequency, 9418 MHz; modulation frequency, 100 kHz; modulation amplitude 1.27 mT, microwave power, 10 dB; temperature, 10 K.

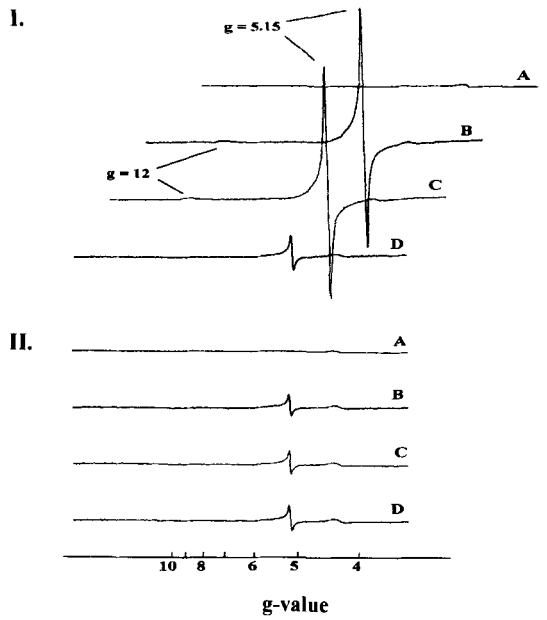

Fig. 8. Low-field spectrum of the high-spin signals of dithionite-reduced benzoyl-CoA reductase (12 mg/ml). (I) Effect of the addition of 10 mM MgATP. The lines point to a second signal appearing at $g = 12$. (A) control without ATP, (B) after 0.5 min, (C) after 5 min, (D) after 10 min incubation with 10 mM ATP. (II) Effect of addition of 10 mM MgADP. (A) Control without ADP, (B) after 0.5 min, (C) after 5 min, (D) after 10 min incubation with 10 mM ADP. The samples in (I) were identical to those of Fig. 6; in experiment (II) the samples were incubated in the presence of ADP analogously to the experiment in Fig. 6. EPR conditions: microwave frequency, 9418 MHz; modulation frequency, 100 kHz; modulation amplitude, 1.27 mT; microwave power, 20 dB; temperature, 28 K. In (I) only the lowest spectrum fits to the g-scale. The other spectra were shifted for better visualization.

EPR-properties of dithionite-reduced and thionine-oxidized benzoyl-CoA reductase. The reversibility of oxidation of the active, reduced enzyme with thionine enabled us to study the EPR properties of the enzyme in different redox states. Dithionite-reduced (10 mM) benzoyl-CoA reductase showed an EPR spectrum at 25 K which looked like an overlap of two signals of reduced Fe-S clusters (Fig. 6). Both signals could easily be observed at 80 K, but optimally sharpened at about 35 K. Two signals, one rhombic ($g_{xyz} = 1.908, 1.95, 2.015$) and one axial ($g_{xyz} = 1.935, 1.935, 2.054$), could be distinguished. With increasing temperatures (above 40 K), the axial signal broadened slightly faster than the rhombic one. At 35 K saturation of both signals set in at microwave powers greater than 20 dB. At 10 K the signals saturated completely at 10 dB. These EPR properties are those of a [2Fe-2S] cluster. Reduced [4Fe-4S] clusters can only be detected below 30–50 K and sharpen optimally at temperatures between 8 K and 20 K. The spin concentration of the sum of both signals was determined against a copper standard and amounted to 0.4 mol/mol enzyme.

At temperatures below 20 K, featureless, very broad signals were detectable which covered about 300 mT of the spectrum around the $g = 2$ region. This spectrum (Fig. 7, trace A) is obtained at 10 K and 10 dB (optimal conditions). The signals of the [2Fe-2S] clusters were nearly completely saturated under these conditions. The remaining spectrum is ascribed to a $S = 1/2$ state of two interacting reduced $[4Fe\text{-}4S]^+$ clusters. The total spin concentration of the combined signals amounted to two spins/enzyme which was in accordance with the assumed presence of two cubanes.

Oxidation of the enzyme with thionine resulted in oxidation of all Fe-S clusters which rendered them diamagnetic (data not shown).

Effect of MgATP and MgADP on EPR properties of benzoyl-CoA reductase. To detect the EPR properties of dithionite-reduced benzoyl-CoA reductase in the steady state of ATPase activity, spectra were recorded at different times after addition of MgATP.

In a time-course experiment the enzyme (12 mg/ml) was incubated for 0.5, 5 and 10 min at room temperature with $Na_2S_2O_4$ (10 mM), $MgCl_2$ (20 mM) and ATP (10 mM). Under the same conditions incubation with MgADP (10 mM) instead of MgATP served as control. In the presence of ATP at least two new signals, at $g = 5.15$ and $g = 12$, were detectable at 25 K (Fig. 6A). The two new signals were already maximally developed after short incubation (0.5 min) and remained constant for at least 5 min. After 10 min incubation the signals were no longer detectable, probably due to loss of the effect of ATP on the enzyme. This was either caused by complete ATP consumption or by accumulation of ADP. The time point of complete ATP consumption due to ATPase activity can be estimated from the known ATP-hydrolysis rate (≈150 nmol ATP min^{-1} mg $protein^{-1}$ at 37 °C) of the enzyme at 8 min incubation. The spectra of the [2Fe-2S] clusters showed no remarkable differences upon addition of MgATP (Fig. 6B). The slight differences in the $g = 2.04-1.97$ region are not understood.

To detect possible effects of MgATP on the two interacting [4Fe-4S] clusters, the same samples as in Fig. 6 were recorded at 10 K and 10 dB (Fig. 7) Addition of MgATP markedly affected the signals from the two interacting $[4Fe\text{-}4S]^+$ clusters, especially after long incubation (10 min). The line shape in the $g = 2$ signal region changed: before ATP addition it was indicative for two interacting cubane clusters and had broad wings (see arrows), but 10 min after addition of MgATP, the signal sharpened considerably. At the same time the double-integrated

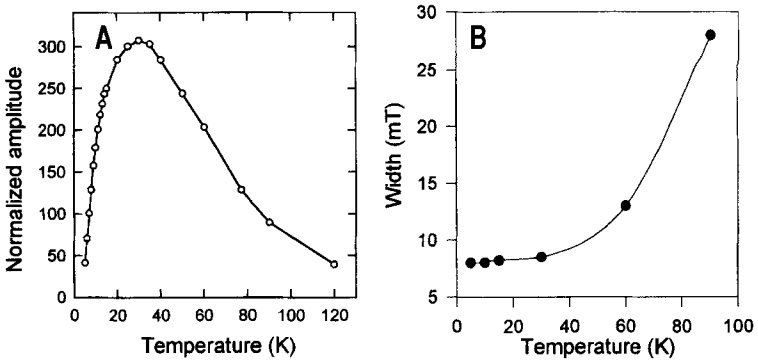

Fig. 9. Characterization of the ATP-induced signal at $g = 5.15$. (A.) Temperature dependence of the amplitude of the signal, normalized for microwave frequency, temperature and gain. EPR conditions: microwave frequency, 9416 MHz; modulation frequency 100 kHz; modulation amplitude 1.27 mT; microwave power 10–30 dB (non-saturating). (B) Temperature dependence of the width of the signal. EPR conditions as in (A) but with a modulation amplitude of 0.32 mT.

intensity of the spectrum in the $g = 2$ region decreased by about 25% (to about 1.5 spin/enzyme molecule). The changes indicate that in the absence of ATP the cubane clusters are fully reduced and show mutual spin-spin interaction. The MgATP-induced spectral change may be a result of partial oxidation of one of the clusters. When oxidized via this route, the cluster is no longer reducible with excess dithionite present in the assay.

Fig. 8(I) shows the low-field part of the spectra from Fig. 6A. The MgATP-induced signal at $g = 5.15$ is very sharp and nearly perfectly isotropic. In controls, where MgATP was replaced by MgADP, only a minor signal at $g = 5.15$ (<5%) appeared upon ADP addition (Fig. 8II). Incubation of the enzyme with ADP also did not influence either the signals of the $[2Fe\text{-}2S]^+$ clusters or those of the $[4Fe\text{-}4S]^+$ clusters.

To further characterize the ATP-induced signal at $g = 5.15$ in the reduced enzyme, its temperature dependence was investigated between 6 K and 120 K (Fig. 9A). We noticed that at 6 K the signal did not show signs of saturation up to 10 dB, so it is a very rapidly relaxing system. The amplitudes of the signal, normalized for microwave power, temperature and gain, were plotted against the temperature. The temperature dependence of the $g = 5.15$ signal showed a maximum (at 32 K). This feature is typical for a signal of an excited state of a high-spin system. While at temperatures below 30 K the excited state became depopulated, at temperatures higher than 30 K the amplitude decreased due to relaxation broadening. Remarkably, this signal at $g = 5.15$ was detectable up to 110 K. The isotropic signal was very sharp with a minimal line width of 0.85 mT at 5 K. The g-values of the lines at $g = 5.15$ and 12 of the MgATP-induced signals are indicative for the lower two doublets of a $S = 7/2$ system [16]. The isotropic signal at $g = 5.15$ gives rise to the theoretically expected isotropic signal of the first excited state doublet of a $S = 7/2$ system at the predicted intermediate rhombicity of $E/D = 0.12$. The weak signal at $g = 12$ is ascribed to the doublet of the ground state. The spectrum showed no additional signals at g-values greater than 4 and we therefore conclude that no other high-spin systems ($S = 3/2$, 5/2, 9/2 and higher) are present [16]. Using the method of Hagen and coworkers [24] and the observed temperature dependence of the $g = 5.15$ signal, a value of 4.3 cm^{-1} could be calculated for the zero-field splitting parameter D. This enabled us to estimate the spin concentration of the system at 28 K [16]. The $g = 5.15$ signal in the dithionite-reduced enzyme in the presence of 10 mM MgATP represented a spin concentration of 3% of the enzyme concentration.

In controls with thionine-oxidized benzoyl-CoA reductase (not shown) the Fe-S clusters apparently were diamagnetic and

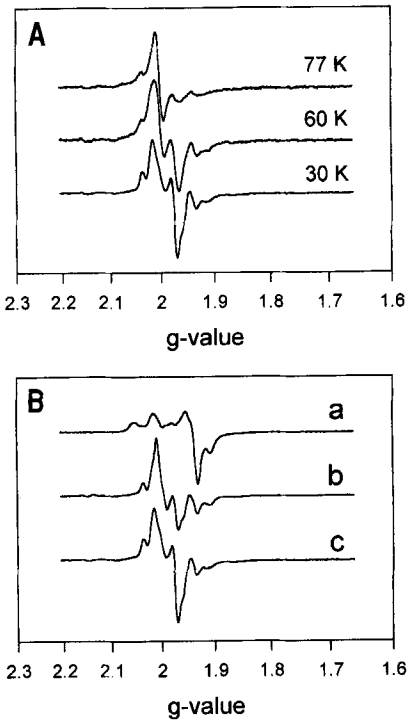

Fig. 10. Effect of benzoyl-CoA and NH_2OH on the EPR-spectra of dithionite-reduced benzoyl-CoA reductase (12 mg/ml). (A) Temperature dependence of the EPR spectra of benzoyl-CoA reductase in the presence of 10 mM $Na_2S_2O_4$, 10 mM MgATP, 20 mM $MgCl_2$ and 2 mM benzoyl-CoA. (B) EPR spectra at 30 K of dithionite (5 mM)-reduced benzoyl-CoA reductase (a) without MgATP and a reducible substrate, (b) with 10 mM MgATP and 2 mM NH_2OH, (c) with 10 mM MgATP and 2 mM benzoyl-CoA. EPR conditions: microwave frequency, 9417 Mhz; modulation frequency, 100 kHz; modulation amplitude, 12.7 mT; microwave power, 20 dB.

no MgATP-induced extra signals were detectable. Obviously thionine oxidation of the enzyme prevented both ATPase activity (shown in Fig. 2A) and the rise of the MgATP-dependent EPR signals at $g = 5.15$ and 12 (data not shown).

Effect of benzoyl-CoA and hydroxylamine on EPR properties of benzoyl-CoA reductase. The effect of benzoyl-CoA or NH_2OH on the EPR properties of the dithionite-reduced enzyme (10 mM dithionite) was tested in the presence and absence of ATP.

Fig. 10A shows the temperature dependence of the signals obtained with 10 mM MgATP and 2 mM benzoyl-CoA after 0.5 min incubation at room temperature. An asymmetric radical-like signal at $g = 2.002$ was already detectable at 77 K. This signal was only slightly saturable even at maximal microwave power (260 mW). With decreasing temperatures the signals of the $[2Fe\text{-}2S]^+$ clusters sharpened up. Comparison of the spectra at 30 K of the reduced enzyme in the presence of all substrates with the spectra of the enzyme in the absence of benzoyl-CoA indicated that the enzyme was largely oxidized in the steady state of substrate reduction (Fig. 10B). The signals of both the $[2Fe\text{-}2S]^+$ clusters (Fig. 10B) and the interacting $[4Fe\text{-}4S]^+$cubanes (not shown) dramatically decreased upon addition of benzoyl-CoA or NH_2OH. Fig. 10B shows that the EPR spectra of benzoyl-CoA reductase in the steady state of catalysis were quite similar, irrespective of whether benzoyl-CoA or NH_2OH was the reducible substrate. No high-spin signals at $g = 5.15$ or $g = 12$ were detectable. Only after long incubation, when benzoyl-CoA or NH_2OH were obviously completely reduced, the two high-spin signals appeared, indicating that the enzyme shifted from reductase (mainly oxidized form) to substrate-independent ATPase activity (mainly reduced form; data not shown). We noticed that the amount of detectable [2Fe-2S] clusters increased more than twofold upon addition of 2 mM benzoyl-CoA to dithionite-reduced enzyme in the absence of ATP. Only the spin concentration but not the line shape of the [2Fe-2S] clusters was affected (data not shown).

DISCUSSION

ATPase activity of benzoyl-CoA reductase. Benzoyl-CoA reductase is the second known enzyme besides nitrogenase which drives electron transfer to the substrate by stoichiometric hydrolysis of ATP. Benzoyl-CoA reductase exhibits ATPase activity in the absence of a reducible substrate [4]. Oxidation of reduced methyl viologen during ATPase activity did not occur indicating that the enzyme, unlike nitrogenase, is unable to reduce protons to H_2. ATPase activity is strictly dependent on the redox-state of the enzyme; upon mild oxidation with thionine, ATPase activity is completely and reversibly lost. Reduction with dithionite restores both benzoyl-CoA reductase activity and ATPase activity of the enzyme. In the absence of benzoate, futile ATP hydrolysis in starving cells might be avoided by an unknown control mechanism which e.g. induces oxidation of benzoyl-CoA reductase.

Inhibition of benzoyl-CoA reductase by ADP and ATP analogs. As in the case of nitrogenase [18], MgADP acts as a competitive inhibitor of MgATP for benzoyl-CoA reductase. This implies that most probably MgATP and MgADP have the same binding site which is also believed to be the case for nitrogenase [18, 19]. The K_i value of MgADP is only about twice as high as the K_m value of MgATP, indicating that benzoyl-CoA reductase activity is effectively regulated by the ATP/ADP ratio of the cell. The ATP analog Ado*P*[NH]*PP* acts as potent inhibitor whereas Ado*P*[CH_2]*PP* has only a little inhibitory effect and only at high concentrations (> 10 mM). This is not surprising since the structural similarities between Ado*P*[NH]*PP* and ATP (relative bond lengths, bond angles and ionisation constants) are much more pronounced than between ATP and Ado*P*[CH_2]*PP* [20]. Ado*P*[NH]*PP* is known as competitive inhibitor for ATP; a typical example is the inhibition of mitochondrial F_1-ATPase by Ado*P*[NH]*PP* at submicromolar concentrations [21]. Ado*P*[NH]*PP* inactivates benzoyl-CoA reductase in a time-dependent manner. It remains to be proven whether ATP can reactivate the Ado*P*[NH]*PP*-inactivated enzyme.

EPR properties of benzoyl-CoA reductase. Benzoyl-CoA reductase contains 10–12 Fe and acid-labile sulfurs and possibly a flavin cofactor. Besides Zn (0.5 mol/mol enzyme), no other metal or selenium has been found in the enzyme. EPR analysis provided some information concerning the iron-sulfur centers of benzoyl-CoA reductase.

In the dithionite-reduced enzyme several signals in the $g = 2$ region were detectable. According to their line-shapes, g-values and temperature dependencies, we ascribe them to two separate non-interacting $[2Fe\text{-}2S]^+$ clusters and two interacting $[4Fe\text{-}4S]^+$ clusters. This is in accord with the iron and acid-labile sulfur analysis.

We should stress that the spectral features cannot be interpreted unambiguously as those of two $[2Fe\text{-}2S]^+$ and two $[4Fe\text{-}4S]^+$ clusters. It may well be that the enzyme may contain novel Fe clusters. To clarify this point further spectroscopic studies under controlled redox conditions and the primary structure of the proteins would be required. The following discussion assumes conventional Fe clusters.

All the clusters became diamagnetic after mild oxidation of the enzyme with thionine, indicating that they were shifted from the +1 to the +2 charge state. In all enzyme preparations an additional radical signal at $g = 2.002$ was detectable. It is not clear yet, whether this radical signal is an artifact or is related to the possible flavin cofactor of benzoyl-CoA reductase. Small resonances of unknown origin around $g = 1.97$ and 2.037 were also observed, especially when MgATP plus benzoyl-CoA were present (Fig. 10B, trace C).

In the steady state of benzoyl-CoA reduction in the complete enzyme assay (10 mM dithionite, 10 mM MgATP and 2 mM benzoyl-CoA) the Fe-S clusters, 2Fe as well as 4Fe clusters, were mostly oxidized and diamagnetic. This suggests that ATP hydrolysis and/or the reduction of the enzyme is the rate-limiting step in the enzyme reaction rather than substrate reduction. Oxidation of the Fe-S clusters occurred irrespective of whether benzoyl-CoA or NH_2OH was present as reducible substrate. However, addition of benzoyl-CoA to the reduced enzyme in the absence of MgATP markedly increased the proportion of reduced [2Fe-2S] clusters from 0.4 spins to a total of 0.9 spins/enzyme molecule. An asymmetric, radical-like signal was present during steady-state reduction of benzoyl-CoA or NH_2OH. Since a radical mechanism was proposed for the reduction of benzoyl-CoA (biological Birch reduction [2, 22]), the radical-like signal might be attributed to a radical intermediate of the substrate or the enzyme. Replacement of benzoyl-CoA or NH_2OH by [*phenyl*-^{13}C]benzoyl-CoA showed no hyperfine splitting in the EPR spectra which should have been observed in the case of a phenyl radical. Buckel and Keese [23] postulated an alternative radical intermediate, a ketyl radical, localized in the thioester carbonyl-group of benzoyl-CoA. It will be interesting to see if [carboxy-^{13}C] benzoyl-CoA has any effect on the EPR spectrum of benzoyl-CoA reductase in the presence of MgATP and dithionite.

Two novel signals at $g = 5.15$ and $g = 12$ were detectable in the absence of substrates upon addition of MgATP to the reduced enzyme. The positions, shapes and temperature dependencies of these signals were assigned to the first excited doublet ($g = 5.15$) and ground doublet ($g = 12$) of a $S = 7/2$ system ($D = 4.3\ cm^{-1}$), consistent with an E/D ratio of 0.12. We expect these signals correspond with ATPase activity of benzoyl-CoA reductase for several reasons. (a) The signals at $g = 5.15$ and $g = 12$ were strictly dependent on MgATP, replacement of MgATP by MgADP revealed only minor signals (< 5% of MgATP induced signals; Fig. 8). (b) ATP induced the signals only in the dithionite-reduced but not in the thionine-oxidized enzyme. Dithionite-reduced benzoyl-CoA reductase exhibits ATPase activity but not the thionine-oxidized enzyme (Fig. 2).

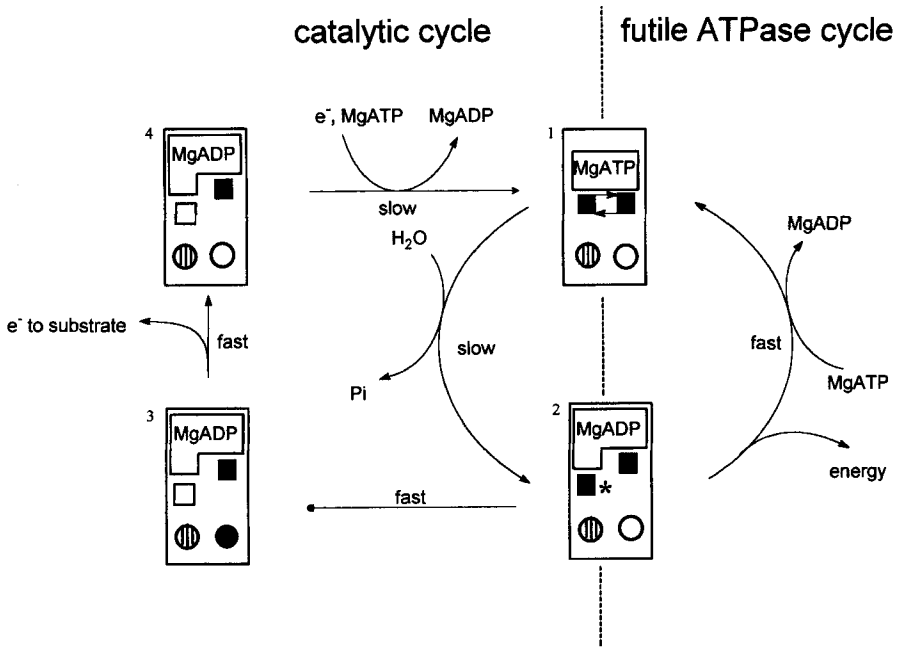

Fig. 11. Proposed simplified catalytic cycle for benzoyl-CoA reductase and ATPase activities of benzoyl-CoA reductase. ■⇄■, two interacting $[4Fe\text{-}4S]^{+1}$ clusters; (■) single non-coupling $[4Fe\text{-}4S]^{1+}$ cluster; (□) $[4Fe\text{-}4S]^{2+}$ cluster, (●) $[2Fe\text{-}2S]^{1+}$ cluster; (○) $[2Fe\text{-}2S]^{2+}$ cluster; (◍) partial population of the reduced [2Fe-2S] cluster; (★) energized electron in a $S = 7/2$ high-spin system. The species 1 and 2 were detected in the steady state of ATPase activity with a spin-concentration ratio of 33:1 (species 1: species 2). In the steady state during reductase activity the enzyme was mostly in the oxidized state (species 4); no $S = 7/2$ high-spin signals were detected. For species 3 no EPR-spectroscopic evidence was available yet. Note that the exact redox states of the [2Fe-2S] clusters during the catalytic cycle are not known yet. The possible involvement of the flavin co-factor in the reaction is not taken into account in this model.

(c) The signals were not present in EPR spectra of enzyme preparations containing dithionite, MgATP and benzoyl-CoA. In the steady state of substrate reduction the enzyme is mainly in the oxidized state and has no substrate-independent ATPase activity. After prolonged incubation the high-spin signals appeared. This may be explained with the observed shifting from reductase (mainly oxidized enzyme) to ATPase activity (mainly reduced enzyme) due to complete substrate consumption (Fig. 4). (d) In time-course experiments in the absence of a reducible substrate but in the presence of MgATP, the intensities of the MgATP-induced signals were maximal after short incubation for 0.5 min and decreased to less than 5% after 10 min incubation. This decrease conforms with the expected decrease of ATPase activity upon prolonged incubation time and may be caused either by the inhibitory effect of accumulated ADP or by depletion of ATP.

The appearance of the two novel signals upon addition of ATP is accompanied by slight changes of the signals of the two [4Fe-4S] clusters. The broad low-field shoulder (see arrow in Fig. 7, traces A and B) diminishes and the lines in the $g = 2$ region become sharper and increase in amplitude. This points to a decrease of the amount of coupling between the two clusters. After 10 min incubation (Fig. 7C), when the $g = 5.15$ and $g = 12$ signals completely disappeared (Fig. 8), three lines of a non-interacting 4Fe cluster can be recognized ($g_{xyz} = 1.86, 1.92, 2.05$). At the same time, the total integrated intensity decreased by 25%. This indicates that one of the formerly interacting clusters can no longer be reduced by dithionite. Since MgADP is supposed to have the same enzyme-binding site as MgATP we conclude that ATP hydrolysis rather than binding of MgATP induces the observed changes. After prolonged incubation, when the ADP/ATP ratio increases in the absence of an ATP regenerating system, the adenosine nucleotide-binding site of the enzyme is thought to be mostly occupied by MgADP. In this phase, we observe the enzyme in a partly oxidized state, indicating that the binding of MgADP might prevent reduction of one of the cubane clusters. The oxidation of the enzyme might be due to an as yet unobserved hydrogenase activity or to a reversal of the reaction with the chemical reductant.

There are only a few reports on high-spin systems iron-sulfur-proteins, especially for systems with $S > 5/2$: for $S = 7/2$ only two [24, 25] and for $S = 9/2$ only a few examples are known [26–28]. In most cases the iron-sulfur clusters have a complex structure as, for example, the P-cluster of MoFe protein of nitrogenase [24] and the hypothetical [6Fe-6S]-cluster-containing protein [26]. In clostridial ferredoxin the high-spin state was obtained by exchanging the acid-labile sulfur for selenium [25]. The dithionite-reduced selenium-substituted ferredoxin exhibits EPR spectra very similar to those of dithionite-reduced benzoyl-CoA reductase in the presence of MgATP with a typical isotropic signal at $g = 5.17$ with E/D = 0.12. The signal was accompanied by signals at $g = 12.76$ and $g = 10.11$ which were ascribed to the doublets of the ground state and the two excited states of a $S = 7/2$ system. The appearence of high-spin signals was attributed to a change in the polypeptide environment of two [4Fe-4S] clusters rather than to selenium substitution [25]. In benzoyl-CoA reductase the spin intensity of the $g = 5.15$ signal amounts to only 3% of the enzyme concentration. In combination with the observation of a slow decrease of overall spin concentration of the cubane clusters, with a concurrent decoupling (Fig. 7), we presently assume that the $S = 7/2$ system arises from one of the cubane clusters by the effect of ATP. We assume an ATP-induced structural change around one of the clusters. We further assume that the $S = 7/2$ state is not stable and becomes slowly oxidized. The low spin concentration might be the result of the balance between the kinetics of formation and oxidation. When oxidizied via this route, the cluster cannot be reduced by the present dithionite.

Stoichiometry and possible role of ATP hydrolysis. 2 ATP/molecule substrate are hydrolysed in the benzoyl-CoA reductase reaction (i.e. 1 ATP/electron transferred), independent of whether benzoyl-CoA or NH_2OH was the substrate. This is in contrast to MgATP-driven reduction of dinitrogen by nitrogenase in which two ATP/electron are hydrolyzed [29].

The role of MgATP in nitrogenase reaction is still not completely clear. Only MgATP-bound Fe protein is able to transfer an electron to the P-cluster of the MoFe protein. Binding of MgATP to the Fe protein lowers the redox-potential of the protein by about 100 mV. However, MgATP hydrolysis is considered to be required for kinetic rather than for thermodynamic reasons, probably by causing conformational changes in both the Fe protein and the MoFe protein of nitrogenase which enable electron transfer [29]. From the data presented here, we assume that ATP-hydrolysis in benzoyl-CoA reductase might decrease the redox potential of one of the reduced [4Fe-4S] clusters by changing the protein structure around it. One of the detectable consequences is a shift of the electronic ground state of the cluster from the $S = 1/2$ state to the $S = 7/2$ state. We also noticed, that in time, one of the Fe-S clusters, presumably the ATP-affected one, became oxidized to an extent of 50%, even though excess dithionite was present. Moreover, as it is considered in nitrogenase [29], MgATP-dependent conformational switches in the enzyme could be necessary to guarantee unidirectional electron transport.

An interesting model for the ATP requirement of benzoyl-CoA reductase is the ATP-dependent reductive activation of (*R*)-2-hydroxyglutaryl-CoA dehydrogenase [4, 30]. A similar initiating step has been proposed for both reactions, namely the α-elimination of water and the ring reduction of CoA-activated acids [23]. The N-terminal amino acid sequences of both enzyme systems show considerable similarities (Boll, M. and Fuchs, G., unpublished results), [31]. This lends strong support to the idea that the (*R*)-2-hydroxyglutaryl-CoA dehydratase system rather than nitrogenase is the most appropriate model for benzoyl-CoA reductase.

Catalytic cycle and rate-limiting steps. In Fig. 11 we present a scheme of the possible events during the catalytic cycle and ATP-hydrolysis. The scheme is highly tentative and serves mainly as working hypothesis for further experiments. It is based on the following considerations. All artificial electron donors are one-electron donors. Therefore we assume a transfer of single electrons via different redox centers to the substrate, very much like in Birch reduction. A futile ATPase cycle and a substrate-reduction cycle occur which are both dependent on the reduced state of the enzyme. ATPase activity is thought to be associated with a transformation of one of the reduced [4Fe-4S] clusters into a low-potential form detectable via a conversion of an $S = 1/2$ state to an $S = 7/2$ state. This effect should be caused by ATP hydrolysis rather than MgATP binding. Since MgADP acts as competitive inhibitor it should bind to the same site as MgATP; however, MgADP does not cause similar EPR-detectable effects as MgATP. Energization of one the [4Fe-4S] cluster into the low-potential form leads to a slow oxidation of the cluster when no reducible substrate is available. It also results in a normal, non-coupled EPR line shape of the other [4Fe-4S] clusters which is not affected. The [2Fe-2S] clusters seem not to be involved in these processes. They might rather play a role in subsequent electron transfer to the substrate or in binding of the substrate, as evidenced by the notable increase of reduction after addition of benzoyl-CoA (in the absence of ATP). This indicates that binding of the aromatic substrate increases the potential of these clusters, whereas the substrate is not reduced under these conditions.

We do not know the order of electron and proton transfer to the substrate. From a thermodynamic point of view, the transfer of the first electron to the substrate may be considered as the rate-limiting reaction; transfer of the second electron might be more favourable. For the scheme shown in Fig. 11 we assume that one ATP is hydrolyzed for each of the two single-electron reduction steps. We cannot exclude the possibility that e.g. only transfer of the first electron is coupled to the hydrolysis of two ATP molecules.

In the steady state of benzoyl-CoA or hydroxylamine reduction the enzyme is mostly in the oxidized state. This suggests that transfer of the excited electron to the substrate is a fast process. We assume that for the overall catalytic cycle the re-reduction of the oxidized enzyme is rate limiting. In the steady state of ATPase activity, we observed only little accumulation (3% of the enzyme concentration) of the signals from the energized [4Fe-4S] cluster. Therefore we assume that ATP hydrolysis is a slower process than the necessary MgADP/MgATP exchange. Otherwise the high-spin signals should be detectable to a higher extent. The rates of the individual partial reactions might be in the order electron transfer to the substrate > MgADP/MgATP exchange > ATP hydrolysis > reduction of the enzyme.

We acknowledge Dr A. J. Pierik for help with the determination of the $S = 7/2$ concentration. S. P. J. A. is indebted to the Netherlands Foundation for Chemical Research (SON), for grants, supplied via the Netherlands Organization for Scientific Research (NWO), which enabled the purchase of the Bruker ECS 106 EPR spectrometer. G. F. is grateful for support by the *Deutsche Forschungsgemeinschaft* (*Schwerpunkt 'Anaerobier'*) and *Land Baden-Württemberg* (Grant 'PWAB') and *Fonds der Chemischen Industrie*. Thanks are due to Dr Johann Heider for reading the manuscript.

REFERENCES

1. Koch, J. & Fuchs, G. (1992) Enzymatic reduction of benzoyl-CoA to alicyclic compounds, a key reaction in anaerobic aromatic metabolism, *Eur. J. Biochem. 205*, 195–202.
2. Koch, J., Eisenreich, W., Bacher, A. & Fuchs, G. (1993) Products of enzymatic reduction of benzoyl-CoA, a key reaction in anaerobic aromatic metabolism, *Eur. J. Biochem. 211*, 649–661.
3. Gibson, K. J. & Gibson, J. (1992) Potential early intermediates in anaerobic benzoate degradation by *Rhodopseudomonas palustris*, *Appl. Environ. Microbiol. 58*, 696–698.
4. Boll, M. & Fuchs, G. (1995) Benzoyl-coenzyme A reductase (dearomatizing), a key enzyme of anaerobic aromatic metabolism. ATP dependence of the reaction, purification and some properties of the enzyme from *Thauera aromatica* strain K172, *Eur. J. Biochem. 234*, 921–933.
5. Heider, J. & Fuchs, G. (1997) Anaerobic metabolism of aromatic compounds, *Eur. J. Biochem.*, in the press.
6. Schachter, D. & Taggart, J. V. (1976) Benzoyl coenzyme A and hippurate synthesis, *J. Biol. Chem. 203*, 925–933.
7. Ziegler, K., Braun, K., Böckler, A. & Fuchs, G. (1987) Studies on the anaerobic degradation of benzoic acid and 2-aminobenzoic acid by a denitrifying *Pseudomonas* strain, *Arch. Microbiol. 149*, 62–69.
8. Tschech, A. & Fuchs, G. (1987) Anaerobic degradation of phenol by pure cultures of newly isolated denitrifying pseudomonads, *Arch. Microbiol. 148*, 213–217.
9. Anders, H.-J., Kaetzke, A., Kämpfer, P., Ludwig, W. & Fuchs, G. (1995) Taxonomic position of aromatic-degrading denitrifying Pseudomonad strains K 172 and KB 740 and their description as new members of the genera *Thauera*, as *Thauera aromatica* sp.nov. and *Azoarcus*, as *Azoarcus evansi* sp. nov., respectively, members of the beta subclass of the Proteobacteria, *Int. J. Syst. Bacteriol. 45*, 327–333.
10. Dawson, R. M. C., Elliott, D. C., Eliott, W. H. & Kenneth, M. J. (1986) *Data for biochemical research*, 3rd edn Clarendon Press, Oxford.

11. Webster, L. T., Mieyal, J. J. & Siddiqui, U. A. (1974) Benzoyl and hydroxybenzoyl esters of coenzyme A. Ultraviolet characterization and reaction mechanisms, *J. Biol. Chem. 249*, 2641–2645.
12. Bradford, M. M. (1976) A rapid and sensitive method for the quantitation of microgram quantities of protein utilizing the principle of protein-dye binding, *Anal. Biochem. 72*, 248–254.
13. Laemmli, U. K. (1970) Cleavage of structural proteins during the assembly of the head of bacteriophage T4, *Nature 227*, 680–685.
14. Zehr, B. D., Savin, T. J. & Hall, R. E. (1989) A one-step, low background coomassie staining procedure for polyacrylamide gels, *Anal. Biochem. 182*, 157–159.
15. Albracht, S. P. J. (1984) Applications of electron paramagnetic resonance in the study of iron sulfur clusters in energy-transducing membranes, *Curr. Top. Bioenerg. 13*, 79–106.
16. Hagen, W. R. (1992) EPR spectroscopy of iron-sulfur proteins, *Adv. Inorg. Chem. 38*, 165–222.
17. Reference deleted.
18. Yates, M. G. (1992) The enzymology of molybdenum-dependent nitrogen fixation, in *Biological nitrogen fixation* (Stacey, G., Evans, H. J. & Burris, R. H., eds) pp. 683–735, Chapman and Hall, New York.
19. Cordewener, J., Haaker, P., van Ewijk, P. & Veeger, C. (1985) Properties of the MgATP and MgADP binding sites on the Fe protein of nitrogenase from *Azotobacter vinelandii*, *Eur. J. Biochem. 148*, 499–508.
20. Yount, R. G. (1975) ATP analogs, *Adv. Enzymol. 43*, 1–56.
21. Gresser, M. J., Beharry, S. & Moennich, D. M. C. (1984) Inhibition of mitochondrial F1-ATPase by adenylyl β,γ-imidodiphosphate, *Curr. Top. Cell. Reg. 24*, 365–378.
22. Brackmann, R. & Fuchs, G. (1993) Enzymes of anaerobic metabolism of phenolic compounds – 4-Hydroxybenzoyl-CoA reductase (dehydroxylating) from a denitrifying *Pseudomonas* species, *Eur. J. Biochem. 213*, 563–571.
23. Buckel, W. & Keese, R. (1995) One electron reactions of CoASH esters in anaerobic bacteria, *Angew. Chem. 107*, 1595–1598.
24. Hagen, W. R., Wassink, H., Eady, R. R., Smith, B. E. & Haaker, H. (1987) Quantitative EPR of an $S = 7/2$ system in thionine-oxidized MoFe proteins of nitrogenase, *Eur. J. Biochem. 169*, 457–465.
25. Gaillard, J., Moulis J.-M., Auric, P. & Meyer, J. (1985) High multiplicity spin states of 2[4Fe-4Se]$^{+}$ clostridial ferredoxins, *Biochemistry 25*, 464–468.
26. Pierik, A. J., Hagen, W. R., Dunham, W. R. & Sands, R. H. (1992) Multi-frequency EPR and high-resolution Mössbauer spectroscopy of a putative [6Fe-6S] prismane-cluster-containing protein from *Desulfovibrio vulgaris* (Hildenborough), *Eur. J. Biochem. 206*, 705–712.
27. Pierik, A. J. & Hagen, W. R. (1991) $S = 9/2$ EPR signals are evidence against coupling between the siroheme and the Fe/S cluster prosthetic groups in *Desulfovibrio vulgaris* (Hildenborough) dissimilatory sulfite reductase, *Eur. J. Biochem. 195*, 505–516.
28. Jetten, M. S. M., Pierik, A. J. & Hagen, W. R. (1991) EPR characterization of a high-spin system in carbon monoxide dehydrogenase from *Methanothrix soehngenii*, *Eur. J. Biochem. 202*, 1291–1297.
29. Howard, J. B. & Rees, M. D. C. (1994) Nitrogenase: a nucleotide-dependent molecular switch, *Annu. Rev. Biochem. 63*, 235–264.
30. Müller, U. & Buckel, W. (1995) Activation of (*R*)-2-hydroxyglutaryl-CoA dehydratase from *Acidaminococcus fermentans*, *Eur. J. Biochem. 230*, 698–704.
31. Bendrat, K., Müller, U., Klees, A. G. & Buckel, W. (1993) Identification of the gene encoding the activator of (*R*)-2-hydroxyglutaryl-CoA dehydratase from *Acidaminococcus fermentans* by gene expression in *Escherichia coli*, *FEBS Lett. 329*, 329–331.